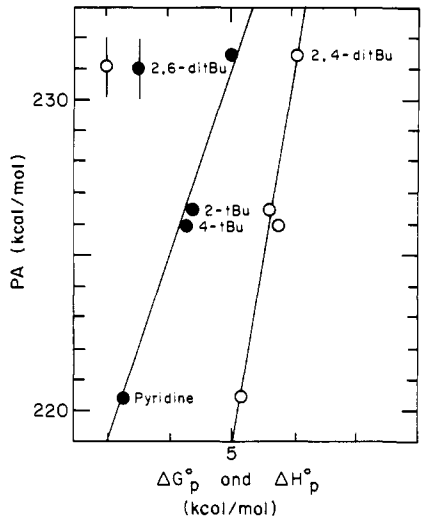

Figure 3. PA plotted vs. $\Delta G_p°$ (○) and $\Delta H_p°$ (●) in 90% methanol–water for a series of *tert*-butyl-substituted pyridines.

for the unusually low basicity of 2,6-DTBP in aqueous solutions.

Correlation of PA and the Basicities in Alcohol–Water Mixtures. Our conclusions derived from the data for the gas phase and aqueous phase can now be compared to a similar analysis of the basicities of *tert*-butyl-substituted pyridines in 90% methanol–water and 40.9% ethanol–water mixtures.[9] Since in these solvent mixtures only pK_a and $\Delta H_p°$ values are available for these compounds, we are restricted to an analysis in which the variations in the basicities in these solvent systems are compared to the corresponding ones in the gas phase. In Figure 3, where PA is plotted vs. both $\Delta G_p°$ and $\Delta H_p°$ for the 90% methanol–water system, one sees that the points for 2,6-DTBP deviate from the linear relationships found for the other pyridines in this study by 1.5 kcal mol^{-1} for $\Delta H_p°$ and by 3.0 kcal mol^{-1} for $\Delta G_p°$. Similar plots for the data in 40.9% ethanol–water have deviations of 2.5 kcal mol^{-1} in $\Delta H_p°$ and only 2.0 kcal mol^{-1} for $\Delta G_p°$. In pure methanol the point for 2,6-DTBP deviates nearly 4.8 kcal mol^{-1} from the linear trend found for PA vs. $\Delta G_p°$, whereas the point for 2,6-diisopropylpyridine deviates from the linear trend by 1.3 kcal mol^{-1}. We note, just as Hopkins and Ali[9] did earlier, that the abnormally low basicity of 2,6-DTBP in these solvents is due apparently to both enthalpy and entropy effects.

Again one is tempted to conclude that the specific solvation of the 2,6-DTBPH$^+$ cation, via hydrogen bonding of a solvent molecule to the pyridine nitrogen, has ceased or at least been reduced substantially. Nevertheless, we easily constructed from CPK models methanol and ethanol hydrogen-bonded complexes for 2,6-DTBP and the 2,6-DTBPH$^+$ cation. In the 2,6-DTBPH$^+$ cation–ethanol complex, steric crowding is much greater than for either the water or methanol complex, which could account for the larger enthalpy effect in the 40.9% ethanol–water mixture. There is, however, uncertainty about which one of the two types of solvent molecules is present in the specific solvation complexes in these mixtures. Actually, both types of hydrogen-bonded complexes could exist in the alcohol–water mixtures for both the neutral pyridines and their cations; thus, there might be different fractions of each type of complex for each of the *tert*-butyl-substituted pyridines. Consequently, further studies must be performed before one can complete a detailed analysis of the basicities of these pyridines in the alcohol–water solvents.

Registry No. 2-TBP, 5944-41-2; 4-TBP, 3978-81-2; 2,4-DTBP, 29939-31-9; 2,6-DTBP, 585-48-8; 2-TBP·H$^+$, 62907-59-9; 4-TBP·H$^+$, 40569-37-7; 2,4-DTBP·H$^+$, 62907-60-2; 2,6-DTBP·H$^+$, 62907-61-3; pyridine, 110-86-1; pyridine·H$^+$, 16969-45-2.

Ab Initio Theoretical Frequencies and Intensities in the Interpretation of Infrared Spectra

B. Andes Hess, Jr.,* L. J. Schaad,* and Prasad L. Polavarapu*

Contribution from the Department of Chemistry, Vanderbilt University, Nashville, Tennessee 37235. *Received January 3, 1984*

Abstract: A comparison of the ab initio theoretical vibrational spectra with the experimental IR spectra of ethylene oxide and its tetradeuterio derivative shows that such calculated spectra can be of use in interpreting experimental results. However, it is crucial that relative intensities be calculated as well as frequencies.

It has been found that ab initio vibrational calculations can be useful in identifying unstable organic species.[1] The comparison of computed[2-5] and experimental spectra of cyclobutadiene and its deuterated derivatives has been useful in resolving the question of its structure (square or rectangular). Similarly, computed IR spectra of thiirene[6,7] have helped confirm its presence in an argon matrix. Since computed frequencies can be in error by as much as a few hundred wavenumbers at short wavelengths, they alone were not sufficient, but when frequencies were combined with computed intensities, fairly definite assignment of observed bands was possible.

In the two cases mentioned the primary purpose of the theoretical work was to aid in picking bands of the molecule sought from others in a reacting mixture. However, theoretical vibrational spectra can also help in interpreting IR bands of pure and otherwise well-characterized molecules. As an example we consider

(1) Hess, B. A., Jr.; Schaad, L. J.; Čársky, P., *Pure Appl. Chem.* **1983**, *55*, 253.
(2) Kollmar, H.; Staemmler, V. *J. Am. Chem. Soc.* **1978**, *100*, 4304.
(3) Schaad, L. J.; Hess, B. A., Jr.; Ewig, C. S. *J. Am. Chem. Soc.* **1979**, *101*, 2281.
(4) Schaad, L. J., Hess, B. A., Jr.; Ewig, C. S. *J. Org. Chem.* **1982**, *47*, 2904.
(5) Hess, B. A., Jr.; Čársky, P.; Schaad, L. J. *J. Am. Chem. Soc.* **1983**, *105*, 695.
(6) Hess, B. A., Jr.; Schaad, L. J.; Ewig, C. S. *J. Am. Chem. Soc.* **1980**, *102*, 2507.
(7) Čársky, P.; Hess, B. A., Jr.; Schaad, L. J. *J. Am. Chem. Soc.* **1983**, *105*, 396.

0002-7863/84/1506-4348$01.50/0

Table I. Symmetry Coordinates[a,b]

species	coordinate
A_1	$S_1 = d$
	$S_2 = 2^{-1/2}(r_1 + r_2)$
	$S_3 = {}^1/_2(t_1 + t_2 + t_3 + t_4)$
	$S_4 = {}^1/_2(\alpha_1 + \alpha_2 + \alpha_3 + \alpha_4)$
	$S_5 = {}^1/_2(\beta_1 + \beta_2 + \beta_3 + \beta_4)$
B_1	$S_9 = 2^{-1/2}(r_1 - r_2)$
	$S_{10} = {}^1/_2(t_1 + t_2 - t_3 - t_4)$
	$S_{11} = {}^1/_2(\alpha_1 + \alpha_2 - \alpha_3 - \alpha_4)$
	$S_{12} = {}^1/_2(\beta_1 + \beta_2 - \beta_3 - \beta_4)$
B_2	$S_{13} = {}^1/_2(t_1 - t_2 - t_3 + t_4)$
	$S_{14} = {}^1/_2(\alpha_1 - \alpha_2 - \alpha_3 + \alpha_4)$
	$S_{15} = {}^1/_2(\beta_1 - \beta_2 - \beta_3 + \beta_4)$

[a] See Figure 1 for definition of internal coordinates. [b] Here, as in ref 8, symmetry species subscript 1 or 2 is determined by symmetry or antisymmetry, respectively, in the plane of the three-membered ring.

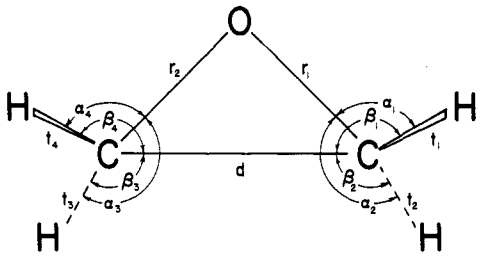

Figure 1. Definition of internal coordinates of ethylene oxide.

ethylene oxide and its tetradeuterio derivative whose experimental IR spectra have been analyzed recently by Nakanaga.[8] Since the errors in variational total energies are large compared to vibrational energies, it is necessary to make such checks of calculated IR spectra for known systems to test the reliability of the theory.[1,3] As our work on these molecules with various basis sets was completed, a paper by Komornicki, Pauzat, and Ellinger[9] appeared with similar results for ethylene oxide but without computations of relative IR intensities. Their work did show the usefulness of theoretical calculations in resolving ambiguities in force constants, particularly off-diagonal terms, obtained by semiclassical means. Thus we shall emphasize the significance of theoretical intensity predictions in vibrational band assignments.

Computational Details

All ab initio calculations were done by using GAUSSIAN 80.[10] The three basis sets STO-3G, 6-31G, and 6-31G* stored in the program were used. Geometry optimizations were carried out at each level by using the Berny gradient method in GAUSSIAN 80. Beginning with the optimized geometry in each basis, each symmetry-adapted internal coordinate in Table I was distorted by 0.01 Å for bond lengths and 3° for angles. Plus and minus distortions were done for those of A symmetry, and single distortions were done for those of B symmetry. The BMAT link of Pulay's program TEXAS[11,13] was used to obtain the Cartesian coordinates of these distorted structures. These were in turn used to compute GAUSSIAN 80 input, and the analytical gradient and dipole moment of each distorted structure were obtained with GAUSSIAN 80 and transformed to the original Cartesian coordinate system generated by BMAT. The BMAT link was utilized to convert the Cartesian gradient for each structure to forces with respect to each internal symmetry coordinate. The matrix of force constants was then computed with these internal forces. A standard Wilson GF analysis gave the vibrational frequencies and their normal modes. Dipole moment derivatives in the direction of the normal mode eigenvectors were computed and gave integrated infrared band intensities as described in ref 7.

Table II. Comparison of Calculated Geometry[a] of Ethylene Oxide with Experiment[b]

parameter	exptl	STO-3G	4-31G[c]	6-31G	6-31G*	6-31G**[c]
r	1.436	1.433	1.459	1.459	1.402	1.399
d	1.472	1.483	1.461	1.464	1.453	1.452
t	1.082	1.088	1.069	1.071	1.077	1.078
α	114.2	116.6	114.5	114.5	115.2	115.4
β	119.4	119.5	119.8	119.8	119.9	119.8

[a] Bond lengths are in Å and angles are in deg. [b] Reference 14. [c] Reference 9.

Table III. 6-31G* Force Constants of Ethylene Oxide[a]

species	constant	value	species	constant	value
A_1	$F_{1,1}$	6.504	B_1	$F_{9,9}$	5.346
	$F_{2,2}$	5.710		$F_{10,10}$	6.194
	$F_{3,3}$	6.199		$F_{11,11}$	1.300
	$F_{4,4}$	1.411		$F_{12,12}$	1.395
	$F_{5,5}$	1.516		$F_{9,10}$	0.508
	$F_{1,2}$	−0.239		$F_{9,11}$	0.655
	$F_{1,3}$	0.139		$F_{9,12}$	−0.298
	$F_{1,4}$	−0.189		$F_{10,11}$	−0.080
	$F_{1,5}$	0.447		$F_{10,12}$	−0.166
	$F_{2,3}$	0.199		$F_{11,12}$	−0.080
	$F_{2,4}$	0.611	B_2	$F_{13,13}$	6.102
	$F_{2,5}$	−0.072		$F_{14,14}$	0.989
	$F_{3,4}$	−0.098		$F_{15,15}$	0.633
	$F_{3,5}$	−0.150		$F_{13,14}$	−0.003
	$F_{4,5}$	−0.175		$F_{13,15}$	0.094
				$F_{14,15}$	−0.282

[a] Stretching force constants are in mdyn Å^{-1}, bending force constants in mdyn Å rad^{-2}, and stretch–bend interaction constants in mdyn rad^{-1}. These force constants are for the symmetry coordinates of Table I.

Table IV. Comparison of Calculated and Experimental[a] Frequencies of Ethylene Oxide[b,c]

symmetry	band	exptl	STO-3G[d]	4-31G[e]	6-31G	6-31G*	6-31G**[e]
A_1	1	3005	3623	3334	3340	3306	3278
	2	1497	1833	1686	1686	1705	1694
	3	1270	1526	1372	1381	1426	1425
	4	1120	1423	1260	1265	1310	1303
	5	877	1097	842	899	992	991
B_1	9	2978	3604	3320	3325	3293	3264
	10	1470	1762	1658	1655	1652	1640
	11	1159	1366	1306	1305	1295	1290
	12	822	1277	862	866	975	978
B_2	13	3065	3773	3431	3440	3394	3367
	14	1147	1308	1236	1235	1290	1286
	15	808	945	909	907	887	885

[a] Taken from ref 8. [b] Frequencies in cm^{-1}. [c] Here, as in ref 8, symmetry species subscript 1 or 2 is determined by symmetry or antisymmetry, respectively, in the plane of the three-membered ring. [d] This work, but in excellent agreement with those reported in ref 9. [e] Reference 9.

Results and Discussion

Optimized Geometry. In Table II the computed geometries of ethylene oxide with various basis sets are compared with experiment. All basis sets give reasonably good agreement with experiment, although the larger basis sets give bond distances which are significantly shorter than experiment as is generally found to be the case. The energies with the STO-3G, 6-31G, and 6-31G* bases are −150.928 50, −152.784 53, and −152.867 35 au respectively.

Force Constants and Frequencies. Calculated force constants (6-31G*) are given in Table III for the symmetry coordinates of Table I. They are not directly comparable with those obtained by Komornicki, Pauzat, and Ellinger since we have used internal

(8) Nakanaga, T. *J. Chem. Phys.* **1981**, *74*, 5384.
(9) Komornicki, A.; Pauzat, P.; Ellinger, Y. *J. Phys. Chem.* **1983**, *87*, 3847.
(10) Binkley, J. S.; Whiteside, R. A.; Krishnan, R.; Seeger, R.; Defrees, D. J.; Schlegel, J. B.; Topiol, S.; Kahn, L. R.; Pople, J. A. GAUSSIAN 80, Quantum Chemistry Program Exchange, Indiana University, Bloomington, IN. We thank Professor John Yates, University of Pittsburgh, for a DEC version of this program.
(11) Pulay, P. *Theor. Chim. Acta* **1979**, *50*, 299.
(12) Pulay, P. *Mol. Phys.* **1969**, *17*, 197.
(13) Pulay, P. In "Modern Theoretical Chemistry"; Schaefer, H. F., III, Ed.; Plenum Press: New York, 1977; Vol. 4, pp 153–185.
(14) Cunningham, G. L.; Jr., Boyd, A. W.; Myers, R. J.; Gwinn, W. D.; Le Van, W. I. *J. Chem. Phys.* **1951**, *19*, 676.

Table V. Comparison of Calculated and Experimental[a] Frequencies of Tetradeuterioethylene Oxide[b,c]

symmetry	band	exptl	STO-3G	6-31G	6-31G*
A_1	1	2204	2665	2441	2417
	2	1312	1627	1420	1489
	3	1013	1301	1117	1125[d]
	4	968	1187	1037	1144[d]
	5	752	874	815	833
B_1	9	2177	2611	2403	2378
	10	1083	1337	1216	1215
	11	900	1205	1025	1021
	12	812	1037	848	956
B_2	13	2322	2811	2564	2532
	14	898	1021	956	1004
	15	577	673	647	632

[a] Taken from ref 8. [b] Frequencies in cm^{-1}. [c] Here, as in ref 8, symmetry species subscript 1 or 2 is determined by symmetry or antisymmetry, respectively, in the plane of the three-membered ring. [d] See discussion in text.

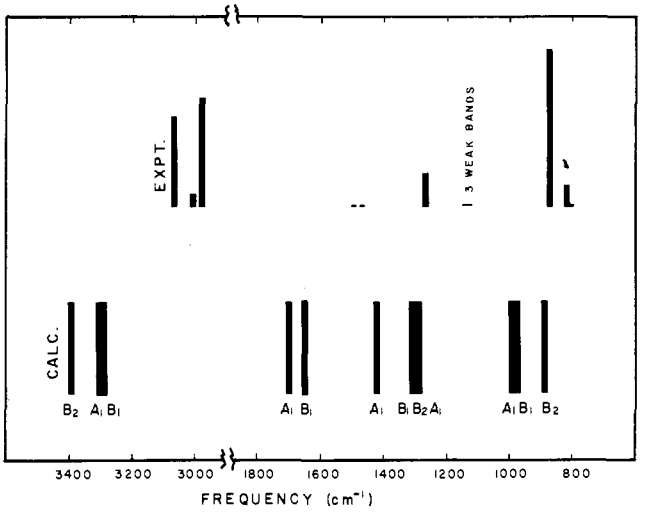

Figure 2. comparison of the experimental spectrum of ethylene oxide with computed (6-31G*) frequencies.

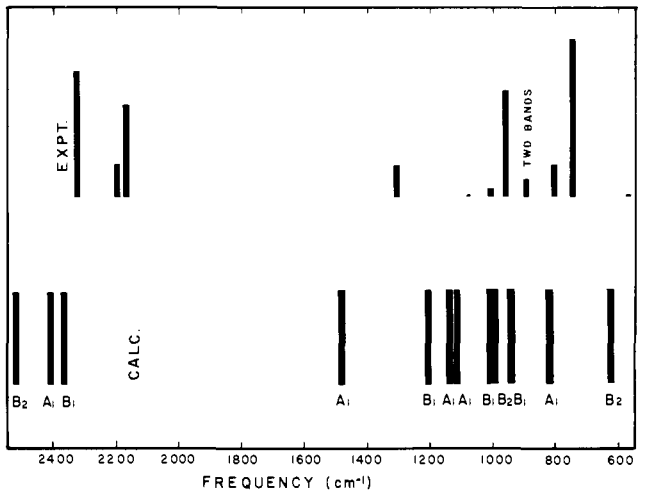

Figure 3. Comparison of the experimental spectrum of tetradeuterioethylene oxide with computed (6-31G*) frequencies.

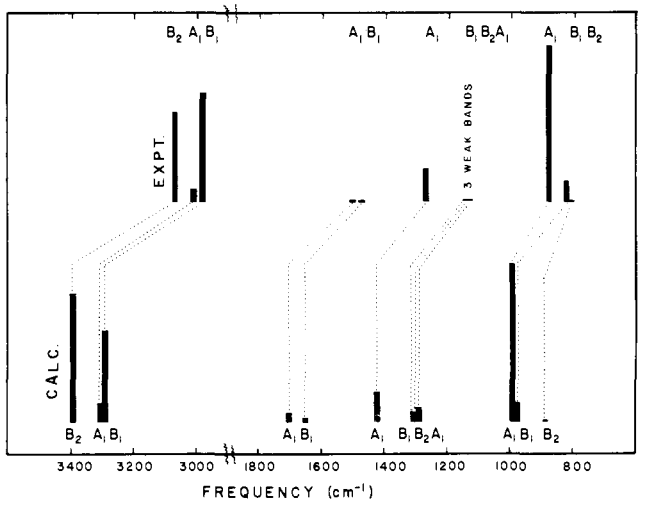

Figure 4. Comparison of the experimental spectrum of ethylene oxide with computed frequencies and intensities (6-31G*).

coordinates different from theirs. However, because of the similarity between our computed frequencies (see below) with the 6-31G* basis and theirs with 6-31G** it is likely that the force constants would compare quite favorably if transformed to the same internal coordinates.

Table IV contains the calculated frequencies of ethylene oxide obtained with five basis sets of increasing size. Examination of these indicates that there are very large differences between the frequencies computed with the STO-3G and the 4-31G bases. Not surprisingly, there is very little difference in those computed with the 4-31G basis and the 6-31G basis since these two bases differ mainly in the treatment of the core electrons. On the other hand addition of polarization functions on carbon and oxygen (6-31G*), while not bringing about significant changes in all the frequencies, does lead to rather large changes in ν_5 and ν_{12}. Finally, addition of polarization functions on the hydrogens (6-31G**) has only a minor effect on the computed frequencies. In Table V we have listed our computed frequencies for the tetradeuterio derivative of ethylene oxide.

Relative Intensities. Computed relative intensities in Table VI are listed along with those from experiment.[8] It is seen that, as with frequencies, there are very significant differences in relative intensities obtained with the STO-3G and 6-31G basis sets. Comparison of the 6-31G and 6-31G* results indicates that relative intensities appear to be somewhat more sensitive to the addition of polarization functions on the carbon and oxygen than do frequencies, but again the differences between the 6-31G and 6-31G* results are much less drastic than those found between the STO-3G and 6-31G results.

Interpretation of Spectra. We deliberately chose to study ethylene oxide because its spectrum has already been reasonably well analyzed experimentally. What we wish to show below is that had both theoretical frequencies and intensities been available earlier they could have aided in the assignment of the infrared bands of ethylene oxide and that therefore such computations should be useful in the future interpretation of experimental vibrational spectra. Hence we shall at first ignore the symmetry assignments made by Nakanaga and demonstrate how the theoretical spectrum could have been used in making these assignments with only the simple IR spectrum of ethylene oxide in hand. We shall proceed with this analysis using our spectrum computed with the 6-31G* basis set.

The experimental spectrum is plotted in Figure 2 along with the 6-31G* frequencies and their symmetry assignments that come directly from the computation; theoretical intensities are not shown. Although all computed frequencies appear to be at significantly higher frequency than experiment, there is some resemblance of the computed spectrum to that of experiment since in both spectra the bands fall into roughly four groupings. However, at this point one would be hesitant to make definite assignments of all bands in the experimental spectrum. For example, in the C–H stretch region two experimental bands (3005 and 2987 cm^{-1}) fall within 27 cm^{-1} of each other. The computed bands lie within 15 cm^{-1} of one another; it would at best be very tenuous to assign the higher of the two to A_1 and the lower to B_1 symmetry. Similarly the three lowest frequency bands in the experimental spectrum lie within a range of 69 cm^{-1}, and the theoretical pattern of this group

Table VI. Comparison of Computed Relative Intensities of Ethylene Oxide and Tetradeuterioethylene Oxide with Experiment[a]

	C_2H_4O				C_2D_4O			
band	exptl	STO-3G	6-31G	6-31G*	exptl	STO-3G	6-31G	6-31G*
1	0.09	0.04	0.03	0.12	0.21	0.03	0.03	0.19
2	0.02	0.01	0.00	0.06	0.19	0.06	0.05	0.39
3	0.21	0.09	0.14	0.19	0.05	0.03	0.03	0.06
4		0.10	0.01	0.06	0.68	0.05	0.23	1.00
5	1.00	0.60	1.00	1.00	1.00	0.69	1.00	0.95
9	0.69	0.78	0.28	0.58	0.58	0.69	0.21	0.71
10	0.01	0.03	0.00	0.02	0.00	0.00	0.00	0.05
11		0.01	0.08	0.00	0.00	0.04	0.08	0.02
12	0.13	0.02	0.06	0.13	0.20	0.02	0.06	0.21
13	0.57	0.03	0.50	0.81	0.69	0.09	0.40	0.99
14		1.00	0.08	0.09	0.11	1.00	0.06	0.10
15	0.00	0.01	0.00	0.00	0.01	0.01	0.00	0.00

[a] Reference 8.

is quite different from that of experiment. Again one would hesitate to make definite symmetry assignments to these three bands.

The inability to make assignments based on computed frequencies alone is even greater in the case of 2,2,3,3-tetradeuterio ethylene oxide as seen from Figure 3. The experimental spectrum has a complex pattern of seven bands between 752 and 1083 cm^{-1}. The computed spectrum also has seven bands between 833 and 1215 cm^{-1}, but the spacing between lines is small compared to the known uncertainty in computed frequencies, and assigning the observed lines on the assumption that the theoretical lines all lie in correct frequency order would be doubtful.

On the other hand when theoretical relative intensities are also considered, many of the above mentioned ambiguities can be resolved. In Figure 4, the theoretical spectrum of ethylene oxide with computed intensities is compared with experiment. It is seen that the two lower bands of the C-H stretch region are computed to be significantly different in relative intensity, which suggests that the symmetries for the three C-H stretches are B_2, A_1, and B_1 from left to the right in the figure. Here the computed frequency order happens to be correct for the closely spaced A_1 and B_1 bands, but the very different intensities make the assignment more certain. Probable assignments can also be made for the next three lower frequency bands as indicated in the figure, though one could not be certain that the B_1 and higher frequency A_1 bands, both of which are weak, might not be reversed. Next appear three weak bands which come very close together. In fact these three bands have not been completely characterized in the experimental spectrum as Nakanaga has noted that "even the frequencies of band centers are not well known".[8] All one would want to conclude from the theoretical numbers is that the weakest of the three should be the B_2. Finally one can now make resonably certain assignments of the lower three bands (as indicated in the figure) when the computed intensities are taken into account. The two bands (A_1 and B_1) which lie very close in frequency in the computed spectrum are very different in computed intensity, which suggests the band at 887 cm^{-1} is A_1 and the one at 822 cm^{-1} is B_1 in the experimental spectrum. This leaves only the very weak band at 808 cm^{-1} which most likely corresponds to the computed B_2 band at 887 cm^{-1}. Here again the computed frequency order happens to be correct, but experimental and theoretical spacings are so different that computed intensities are needed to be sure.

The symmetry assignments made by Nakanaga from his analysis of the experimental spectrum are shown at the top of Figure 4; they are in complete agreement with those deduced by comparing theoretical and experimental spectra.

The computed spectrum of tetradeuterioethylene oxide is compared with experiment in Figure 5. The four highest and one lowest frequencies can be readily assigned to B_2, A_1, B_1, A_1, and B_2, as shown in the figure. There remains the complex pattern of seven lines. Comparison of the computed pattern with that of experiment suggests that the ordering in the one is identical with that in the other, with the exception of the ν_3 and ν_4 bands of A_1 symmetry. Fortunately the large difference in their intensities in both spectra indicates a probable reversal in order

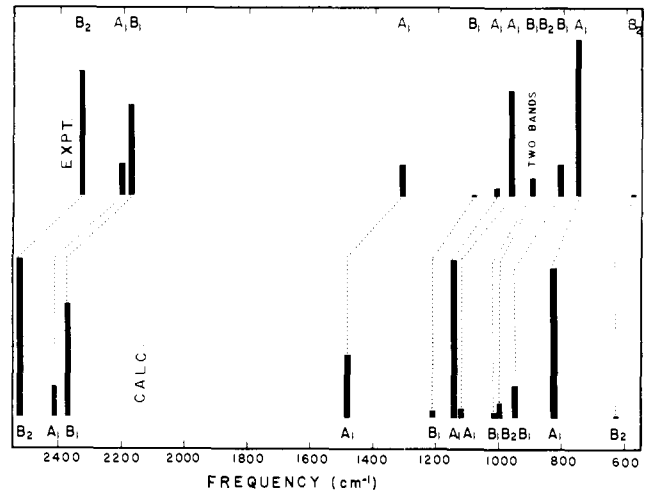

Figure 5. Comparison of the experimental spectrum of tetradeuterioethylene oxide with computed frequencies and intensities (6-31G*).

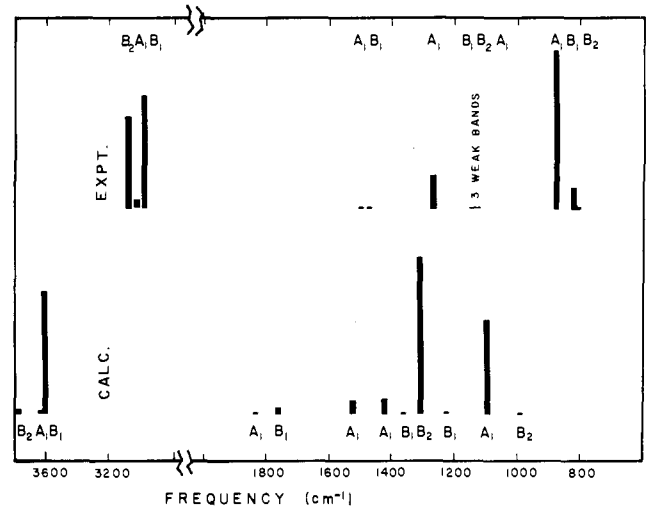

Figure 6. Comparison of the experimental spectrum of ethylene oxide with computed frequencies and intensities (STO-3G).

between the two spectra as indicated. This assignment would certainly not have been possible if the relative intensities were not taken into account. Again our assignments based on the computed spectrum are in complete agreement with those made by Nakanaga. We have also carried out a calculation in which the 6-31G* diagonal force constants were scaled by a factor of 0.9 with the off-diagonal constants left unscaled as recommended by Komornicki, Pauzat, and Ellinger. This did not interchange the computed order of ν_3 and ν_4.

A similar analysis using the 6-31G results of both compounds leads one to the same assignments as with the 6-31G* spectra but

with a lesser degree of certainty for several bands in both spectra, due primarily to poorer computed relative intensities. On the other hand, as Figure 6 shows, even with computed intensities it is seen that at the STO-3G level the assignment of bands in the experimental spectra is essentially hopeless.

This comparison of the theoretical IR spectra with the well-characterized spectra of ethylene oxide has shown that computed frequencies and intensities should aid in the interpretation of less well-characterized spectra of small molecules.

Acknowledgment. This work was supported by a grant (GM29375) from NIH to one of us (P.L.P.).

Registry No. Ethylene oxide, 75-21-8; tetradeuterioethylene oxide, 6552-57-4.

The Dynamics of the Photochemical Decarbonylation of 3-Cyclopentenone

Blake I. Sonobe, T. Rick Fletcher, and Robert N. Rosenfeld*

Contribution from the Department of Chemistry, University of California, Davis, California 95616. *Received January 6, 1984*

Abstract: 3-Cyclopentenone undergoes photofragmentation, yielding butadiene and CO. The dynamics of this reaction have been investigated by using the method of time-resolved CO laser absorption spectroscopy. Nascent CO product vibrational energy distributions are directly determined. Dissociation at 193 nm yields CO with $N_0:N_1:N_2:N_3:N_4 = 1.00:0.30:0.11:0.04:0.01$, dissociation at 249 nm yields CO with $N_0:N_1:N_2 = 1.00:0.24:0.03$, and dissociation at 308 nm yields CO with $N_0:N_1 = 1.00:0.02$. The experimental distributions are analyzed by comparing them with distributions calculated by using a statistical model. On this basis, we conclude that only the nonfixed energy of the transition state is available for partitioning among the products' vibrational degrees of freedom and that the products are vibrationally decoupled from one another in the exit channel. Potential energy is thus released in the exit channel primarily to the relative translational motion of the products.

Photofragmentation reactions are of interest in the study of elementary reaction dynamics, in part because reactant activation can be accomplished, in the absence of collisions, to a well-defined total energy. This situation greatly simplifies the interpretation of experimental data on product translational, rotational, and vibrational energy distributions so that rather complete pictures of the photodissociation chemisty of small molecular species, e.g., tri- or tetraatomics, have begun to emerge.[1] This is not, however, the case for larger polyatomic systems where the increased number of internal degrees of freedom can introduce additional mechanistic and dynamical possibilities. For example, nonradiative electronic relaxation often competes favorably with direct dissociation in large polyatomics. Similarly, intramolecular vibrational relaxation can be rapid relative to dissociation so that the observed reaction dynamics reflect (microcanonical) ensemble-averaged behavior rather than that of a single ro-vibronic level. Studies of the photofragmentation dynamics of polyatomic molecules can provide some insight as to when such effects are important. The distribution of available energy among dissociation products' various degrees of freedom can yield information on transition-state structure and exit channel effects[2] (i.e., how do the separating products interact with one another). In this paper, we describe recent work from our laboratory on the photofragmentation of 3-cyclopentenone, eq 1, in the gas phase.[3] Energy partitioning

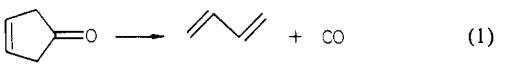

(1)

to the carbon monoxide product is probed by using the technique of time-resolved CO laser absorption spectroscopy. A physical model for the dissociation process is developed in terms of the shape of the reaction's potential surface.

The CO laser absorption method used here has been employed by other workers in studies of photodissociation dynamics.[4,5] Their results, in conjunction with those reported here, constitute a basis for developing detailed mechanistic/dynamical descriptions of elementary photofragmentation processes and provide bench-mark data with which the predictions of emerging ab initio techniques in dynamics may be compared.

Experimental Section

The instrumentation employed for CO laser absorption spectroscopy is illustrated schematically in Figure 1. 3-Cyclopentenone was slowly flowed through a 1-m absorption cell either neat at 0.08–0.5 torr or diluted in argon. Some care was taken to ensure that the reactant pressure was sufficiently low that a "thin target" approximation was valid. The absorption cell was equipped with CaF_2 windows mounted at Brewster's angle. The ketone was photoactivated with an excimer laser (Lambda Physik EMG 101; pulse width ca. 15 ns) using the XeCl*, KrF*, or ArF* transitions at 308, 249, or 193 nm, respectively. Laser fluences were typically 1–5 mJ/cm^2. The TEM_{00} output of a grating tuned, continuous wave (CW) CO laser was copropagated through the absorption cell coaxially with respect to the excimer laser. The CO laser was designed to optimize output on the $(1 \rightarrow 0)$ vibrational transition,[6] where 5–8 mW could be routinely obtained. Appreciably more power was available when the laser was tuned to other vibrational transitions. The CO laser intensity transmitted through the absorption cell was monitored with a 2-mm diameter InSb detector. CO formed in the absorption cell by the photodissociation of 3-cyclopentenone produces a transient decrease in the CO laser intensity reaching the detector. The corresponding detector signal was amplified and then digitized with a Biomation 8100 transient recorder. The detection system rise time was $\lesssim$100 ns. The digitized signal was accumulated in a microcomputer for signal averaging. Typically, 500 transients were averaged. CO product vibrational distributions were determined by recording absorption curves with successive CO laser vibrational transitions until no further absorption could be detected. The CO laser grating drive was calibrated by using a 0.6-m monochromator to determine laser line wavelengths.

In all our experiments, sample pressures were measured with a capacitance manometer, and laser power or pulse energy was determined by using a Scientech power/energy meter. For each UV excitation wave-

(1) Leone, S. R. *Adv. Chem. Phys.* **1982**, *50*, 255.
(2) Polanyi, J. C. *Acc. Chem. Res.* **1972**, *5*, 161.
(3) Sonobe, B. I.; Fletcher, T. R.; Rosenfeld, R. N., submitted for publication in *Chem. Phys. Lett.*
(4) Houston, P. L.; Moore, C. B. *J. Chem. Phys.* **1976**, *65*, 757.
(5) Fujimoto, G. T.; Umstead, M. E.; Lin, M. C. *Chem. Phys.* **1982**, *65*, 197.
(6) Djeu, N. *Appl. Phys.* **1973**, *23*, 309.
(7) Siebert, D. R.; Grabiner, F. R.; Flynn, G. W. *J. Chem. Phys.* **1974**, *60*, 1564.

0002-7863/84/1506-4352$01.50/0